

## Accepted Manuscript

Optimization of taste-masking on ibuprofen microspheres with selected structure features

Wei Qin , Yuanzhi He , Zhen Guo , Liu Zhang , Li Wu ,  
Xianzhen Yin , Shailendra Shakya , Abi Maharjan , Yan Tang ,  
Weifeng Zhu , Jiwen Zhang

PII: S1818-0876(18)30070-9  
DOI: [10.1016/j.ajps.2018.05.003](https://doi.org/10.1016/j.ajps.2018.05.003)  
Reference: AJPS 522



To appear in: *Asian Journal of Pharmaceutical Sciences*

Received date: 24 January 2018  
Revised date: 25 March 2018  
Accepted date: 21 May 2018

Please cite this article as: Wei Qin , Yuanzhi He , Zhen Guo , Liu Zhang , Li Wu , Xianzhen Yin , Shailendra Shakya , Abi Maharjan , Yan Tang , Weifeng Zhu , Jiwen Zhang , Optimization of taste-masking on ibuprofen microspheres with selected structure features, *Asian Journal of Pharmaceutical Sciences* (2018), doi: [10.1016/j.ajps.2018.05.003](https://doi.org/10.1016/j.ajps.2018.05.003)

This is a PDF file of an unedited manuscript that has been accepted for publication. As a service to our customers we are providing this early version of the manuscript. The manuscript will undergo copyediting, typesetting, and review of the resulting proof before it is published in its final form. Please note that during the production process errors may be discovered which could affect the content, and all legal disclaimers that apply to the journal pertain.

**Original Research Paper****Optimization of taste-masking on ibuprofen microspheres with selected structure features**

Authors:

Wei Qin<sup>a,b,1</sup>, Yuanzhi He<sup>a,b,1</sup>, Zhen Guo<sup>b,1</sup>, Liu Zhang<sup>b,c</sup>, Li Wu<sup>b</sup>, Xianzhen Yin<sup>b</sup>,  
Shailendra Shakya<sup>b,d</sup>, Abi Maharjan<sup>b,d</sup>, Yan Tang<sup>a,b</sup>, Weifeng Zhu<sup>a,\*</sup>, Jiwen Zhang<sup>a,b,\*</sup>

Affiliations:

<sup>a</sup> Jiangxi University of Traditional Chinese Medicine, Nanchang 330004, China

<sup>b</sup> Shanghai Institute of Material Medica, Chinese Academy of Science, Shanghai  
201203, China

<sup>c</sup> Department of Pharmaceutical Analysis, School of Pharmacy, Shenyang  
Pharmaceutical University, Shenyang 110016, China

<sup>d</sup> University of Chinese Academy of Sciences, Beijing 100049, China

<sup>1</sup> These authors contributed equally to this work.

\*Corresponding Author. Jiwen Zhang. Address: Shanghai Institute of Materia Medica,  
Chinese Academy of Sciences, 501 Haik Road, Shanghai 201210, China. Fax:  
+86-21-20231980. E-mail: jwzhang@simm.ac.cn. Weifeng Zhu. Address: Jiangxi  
University of Traditional Chinese Medicine, 818 Xingwan Road, Nanchang 330004,  
China. Tel/Fax: +86-791-87118614. E-mail: zwf0322@126.com.

**ABSTRACT**

The microsphere was a primary particulate system for taste-masking with unique structural features defined by production process. In this article, ibuprofen lipid microspheres of octadecanol and glycerin monostearate were prepared to mask the undesirable taste of ibuprofen via three kinds of spray congealing processes, namely, air-cooling, water-cooling and citric acid solution-cooling. The stereoscopic and internal structures of ibuprofen microspheres were quantitatively analyzed by synchrotron radiation X-ray micro-computed tomography (SR- $\mu$ CT) to establish the relationship between the preparation process and microsphere architectures. It was found that the microstructure and morphology of the microspheres were significantly influenced by preparation processes as the primary factors to determine the release profiles and taste-masking effects. The sphericity of ibuprofen microspheres congealed in citric acid solution was higher than the other two and its morphology was more regular than that being congealed in air or distilled water, and the contact angles between congealing media and melted ibuprofen in octadecanol and glycerin monostearate well demonstrated the structure differences among microspheres of three processes which controlled the release characteristics of the microspheres. The structure parameters like porosity, sphericity, and radius ratio from quantitative analysis were correlated well with drug release behaviors. The results demonstrated that the exterior morphology and internal structure of microspheres had considerable influences on the drug release behaviors as well as taste-masking effects.

**Keywords**

Ibuprofen microsphere,

Spray congealing,

Internal structure,

Synchrotron radiation X-ray micro-computed tomography

## 1. Introduction

Taste-masking had great importance for active pharmaceutical ingredients with an unpleasant taste in pediatric medicines as well as for the sensitive patient population. Recently, many taste-masking technologies had been developed, such as spray congealing [1], hot-melt extrusion [2-4], mixing with flavors and sweeteners [5-7], complexation with ion exchangers and cyclodextrins [8-10], encapsulation into microspheres and microcapsules [11], physical barriers or coating [12-14], solid dispersions [15], and granulation [16]. Many microencapsulation processes were modifications of three basic techniques, namely solvent extraction/evaporation, phase separation (coacervation) and spray congealing. However, solvent extraction/evaporation and coacervation were impaired by residual solvents and coacervation agents found in the products ran safety risks for their applications [17]. Therefore, spray congealing that was relatively simple and possess high throughput was usually much safer.

Basically, the aim of taste-masking was to reduce or inhibit the interaction between the active ingredients and the taste buds in tongue. Since the interaction of the dissolved drug molecules with the taste receptors in the human taste buds caused taste reaction, the measurement of the moiety of drug released or dissolved in

simulated oral cavity conditions was an indicator to the taste-masking effects [18].

Furthermore, the morphology was one of the primary factors governing the rate and mechanism of the drug release from solid dosage forms, such as surface and shape of the dosage form. For instance, the rough surface of microspheres often showed faster release rate than the smooth microspheres [19]. The strong relationship between the morphology of the pellets and the value of the mean dissolution time (MDT) had been established [20].

Besides drug release tests, other conventional methods had been employed for micro-particle evaluations, such as optical microscopy for size analysis [21], scanning electron microscopy (SEM) for morphology detection[22], transmission electron microscopy (TEM) for porosity analysis [23], differential scanning calorimetry (DSC) for thermodynamic determination, and X-ray powder diffraction (XRPD) for crystal evaluation [24]. These methods could only evaluate taste-masked products to some extent and were difficult to identify the internal microstructure's roles in taste-masking. Therefore, a quantitative structure characterization method had especial importance to correlate the detail structural information of microspheres with the drug release behaviors, providing new mechanistic knowledge for taste-masking technologies.

Synchrotron radiation X-ray micro-computed tomography (SR- $\mu$ CT), a powerful non-invasive investigation technique for the internal three dimension (3D) structures for various objects, had great potential for quantitative evaluation and design of solid drug delivery systems. The interior porous channels and irregular structures could be

obtained by SR- $\mu$ CT, which could be further correlated with the drug release kinetics of felodipine osmotic pump tablets [25]. On one hand, the surface morphology and the internal 3D structure of felodipine osmotic pump tablets could be visualized; on the other hand, the intrinsic drug release kinetics and 3D parameters, such as surface areas of the remaining core inside the film, could be quantitatively elucidated using SR- $\mu$ CT [26]. Combined with statistical method, SR- $\mu$ CT was used to non-destructively investigate the mixing and segregation of granular materials in 3D [27]. Additionally, SR- $\mu$ CT was also applied for structural analysis of polymer-coated granules and spherical hollow excipients on tableting [28].

As a widely used nonsteroidal anti-inflammatory drug, ibuprofen is rapidly and completely absorbed in the gastrointestinal tract after oral administration. Strong pungent taste of ibuprofen must be masked for the sensitive patients. In this study, ibuprofen lipid microspheres prepared by spray congealing in different cooling media were examined by SR- $\mu$ CT to uncover the internal 3D structures in line with taste-masking. The primary objectives were to study the microstructural basis of lipid microspheres for taste-masking and to provide new evaluation method for production process optimization during taste-masking.

## **2. Materials and methods**

### **2.1. Materials**

Ibuprofen with purity of 99.45% was provided by Hunan Erkang Pharmaceutical Co., Ltd., China. Glycerin monostearate (GMS) and octadecanol, as the excipients for taste-masking were supplied by Hunan Erkang Pharmaceutical Co., Ltd., China.

Sodium phosphate monobasic dehydrate, sodium hydrogen phosphate and phosphoric acid were obtained from Sinopharm Chemical Reagent Co., Ltd., China.

Ibuprofen microspheres were prepared using a spraying technique (Spray gun, W-71, Iwata, Japan). The dissolution test was performed using a dissolution apparatus (ZRS-8G, Tianjin Haiyida Co., Ltd., China). The SR- $\mu$ CT scans were carried out at the Shanghai Synchrotron Radiation Facility (SSRF) in Shanghai Institute of Applied Physics, Chinese Academy of Sciences. Data were analyzed using the commercially available software VGStudio Max (version 2.1, Volume Graphics GmbH, Germany), Image-pro Plus (version 6.0, Media Cybernetics, Inc., Bethesda, MD, USA), Amira (version 5.4.3, Visage Imaging, Inc., Australia) and Image Pro analyzer 3D (version 7.0, Media Cybernetics, Inc., Bethesda, MD, USA).

## **2.2. Preparation of ibuprofen microspheres**

The formulas of ibuprofen microspheres were selected by screening the ratio of ibuprofen, octadecanol, and GMS. According to the morphology, flowability, and dissolution in media of microspheres, the ratio of ibuprofen, octadecanol, and GMS at 3:6:1 (w/w/w) was the best formula. Microspheres were prepared by heating appropriate amount of GMS and octadecanol to 65-70 °C until melted. Then, ibuprofen was gradually added and melted whilst stirring at 500 rpm by a magnetic heated stirrer (ETS-D5, IKA, Germany) to get a uniform mixture. The mixture was immediately poured into the reservoir of spray gun preheated to 70 °C in a dry oven and sprayed. The air-cooling microspheres were collected from stainless steel trays. The water and citric acid solution (pH = 1.20) were also used as cooling media, while

the cooled microspheres were quickly formed in 1000 mL of corresponding medium by a position of spraying at 5 cm above the medium. It was then filtered and dried in a vacuum oven at 40 °C. The microspheres were collected and stored in desiccator for further study. The microspheres were named as ACM, WCM and CCM for air-cooling microspheres, water-cooling microspheres, and citric acid solution-cooling microspheres, respectively.

### **2.3. Contact angle measurement**

The contact angles between water, citric acid solution (pH = 1.20) and ibuprofen microspheres were determined under ambient temperature by a goniometry method. The same as the preparation of ibuprofen microspheres, appropriate amounts of GMS and octadecanol were heated to 65 - 70 °C and ibuprofen was gradually added and melted whilst stirring at 500 rpm to get a uniform mixture. The mixture was immediately poured onto a watch-glass and was cooled to form a uniform film. An appropriate size of film was selected and was put on a horizontal table. Approximately 20  $\mu$ L of the congealing media, namely, water or citric acid solution were deposited on the film from a consistent height. After the drop reached a quasi-equilibrium shape, photos were taken immediately by a camera and were analyzed using Image-pro Plus (version 6.0, Media Cybernetics, Inc., Bethesda, MD, USA) to calculate the contact angle. All measurements were repeated in triplicate by three individual films.

### **2.4. Thermogravimetric analysis**

The thermogravimetric analysis (TGA) measurements were performed by a PerkinElmer Thermogravimetric analyzer Pyris 1 TGA at 10 °C/min in the nitrogen



atmosphere. Samples (approx. 5 mg) were weighed in a hanging aluminum pan and the weight loss percentage of the samples was monitored from 25 to 500 °C. In order to compare the TGA profiles of various samples, the raw data of TGA were re-drawn.

## 2.5. X-ray powder diffraction

The crystallinity of the samples was characterized by X-ray powder diffraction (XRPD). The diffraction patterns were detected with a Bruker D8-ADVANCE X-ray diffractometer (Bruker, Germany) using Cu-K $\alpha$  radiation ( $\lambda=1.54056 \text{ \AA}$ ) at ambient temperature (20 °C). The voltage and current were 40 KV and 40 mA, respectively. Reflection mode was used in the  $2\theta$  range 3-40 ° with a scan speed of 15 °/min (step size 0.025 °, step time 0.1 s) by a lynxEye detector.

## 2.6. Drug release in different media

For the *in vitro* dissolution test to imitate pH conditions *in vivo*, microspheres containing 200 mg ibuprofen in fraction with particle size between 125 and 212  $\mu\text{m}$  were sieved by 70 to 115 mesh screen and were assessed in sextuple for each batch of microspheres. Dissolution tests were performed using the paddle method according to the Chinese Pharmacopoeia 2015 with the rotation speed of 100 rpm. A volume of 900 mL for the distilled water, hydrochloric acid solution (pH = 1.20) or phosphate buffer (pH = 6.80 and 7.20) were used as the dissolution media at  $37 \pm 0.5 \text{ }^\circ\text{C}$ . Aliquots of 2 mL of solution samples were withdrawn at 10, 30, 60, 90, 120, 180, 240, 300, 600 s and an equal volume of the fresh medium with same temperature was added immediately.

The aliquot samples were immediately filtered through a 0.22  $\mu\text{m}$  membrane and

quantified on an HPLC-UV system that consisted of an Agilent 1260 series HPLC system (Agilent Technologies Inc., China) coupled to an Agilent 1290 UV detector. Samples were examined by a Dikma Spursil C18 column (250 mm × 4.6 mm, 5 μm, Phenomenex, USA) at 25 °C. The mobile phase was consisted of sodium acetate buffer (pH = 2.5) and acetonitrile (30:70, v/v). Elution was performed at 25 °C at a flow rate of 1 mL/min. The detection wavelength was set at 263 nm.

### **2.7. Conventional morphology characterization**

All the kinds of microspheres collected during dissolution tests at 0, 5, 10 min were investigated by conventional morphology characterization of scanning electron microscope (SEM, S-3400, Hitachi). The specimens were immobilized on a metal stub with double-sided adhesive tape. The microsphere samples at dissolution time of 5 min and 10 min were grinded gently before measurement, so as to collect the images of internal surfaces from the broken microspheres.

### **2.8. Synchrotron radiation X-ray micro-computed tomography measurement**

To characterize the microstructure of microspheres, SR-μCT images were acquired with beamline BL13W1 at SSRF. The propagation-based imaging (PBI) method was used for the phase contrast imaging to investigate the distribution of low Z materials in the microspheres. Samples were scanned at 13.0 KeV for the higher flux to reduce the imaging time. After penetration through the sample, the X-rays were converted into visible light by a Lu<sub>2</sub>SiO<sub>5</sub>: Ce scintillator (10 mm thickness). Projections were magnified by diffraction-limited microscope optics (10 magnification) and digitized by a high-resolution 2048 pixel × 2048 pixel sCMOS

camera (ORCA Flash 4.0 Scientific CMOS, Hamamatsu K.K, Shizuoka Pref., Japan). The pixel size was 0.65  $\mu\text{m}$ , the sample-to-detector distance was 12.0 cm and the exposure time was 1 s. For each acquisition, 1440 projection images were captured. Flat-field and dark-field images were also collected during each acquisition procedure to correct the electronic noise and variations in the X-ray source brightness.

## 2.9. Three-dimension structure reconstruction

The two-dimension (2D) projection CT scanning transmission images were acquired and analyzed after optimization, noise reduction, shading and segmentation to evaluate preliminarily the effect of imaging and the imaging parameters were optimized. At the same time, the absorption of X-ray of different samples was obtained to qualitatively compare the structural architecture of samples. Based on a series of 2D projection images of different angles, slice images were acquired by reconstructing through X-TRACT software (CSIRO, Commonwealth Scientific and Industrial Research Organization, Australia, <http://www.ts-imaging.net>) to perform a directly filtered back projection algorithm. Slice images were noise-reduced and optimized to improve the discrimination of different substances and density region. From the analysis of gray values, SR- $\mu\text{CT}$  data from all of the microspheres in the samples were examined. Highly resolved tomographic images of voids within microspheres with high-quality phase contrast were then derived after 3D reconstructions.

In total, 30 microspheres were randomly selected from each kinds of microspheres, which were 3D reconstructed using Image-pro Plus (version 6.0, Media

Cybernetics, Inc., Bethesda, MD, USA), Amira (version 5.4.3, Visage Imaging, Inc., Australia) and Image Pro Analyzer 3D (version 7.0, Media Cybernetics, Inc., Bethesda, MD, USA) to quantitatively characterize and visualize the details of internal voids within microspheres.

### **2.10. Statistical data analysis**

Analysis of variance (ANOVA) was performed using SPSS version 21.0 for windows (SPSS Inc., Chicago, the United States) for employing an error probability at  $P \leq 0.05$  for experimental data differences. For each parameter, WCM and CCM were compared with ACM by Student's t-Test.

## **3. Results and discussion**

### **3.1 Contact angle**

Approximately 20  $\mu\text{L}$  water or citric acid solution were deposited on the film, there was significant difference in the quasi-equilibrium shape of drops. The drop of water had a smaller contact angle than that of citric acid solution with contact angle of  $71.94 \pm 1.20^\circ$ ,  $80.97 \pm 2.22^\circ$ , respectively. The surface of film representing the surface of ibuprofen microspheres was hydrophilic due to the contact angle less than  $90^\circ$ . It also indicated that ibuprofen microspheres had a better wettability in water owing to lower contact angle. According to the equation Yang, the greater contact angle means larger interfacial tension. A high interfacial tension may generate more typical spherical morphology and high porosity in ibuprofen microspheres congealed in citric acid solution.

### **3.2. Thermal gravimetric analysis**

GMS showed three-stage weight loss, the first weight loss at around 120-215 °C relating to the weight loss of moisture, second weight loss at the temperature range of 220- 325 °C correlating to the decomposition of ester bond of GMS and final weight loss at 350-420 °C might be due to the carbonization of intermediate products. Ibuprofen and octadecanol performed single-step weight loss at around 120-228 °C relating to the thermal oxidation reaction. For microspheres, the single-step mass loss were at the temperature range of 120- 226 °C, 120-258 °C and 120-254 °C for ACM, WCM and CCM, respectively. Overall, it was indicated that the thermal decomposition of all the samples occurred above 120 °C, which proved the stability of constitutions of microspheres at lower temperature during the preparation process (Fig. 1).

### 3.3. X-ray powder diffraction

It was indicated that ibuprofen, octadecanol, and GMS were crystals (Fig. 2). The characteristic peaks for ibuprofen were normalized to invariable peaks of octadecanol and GMS which were insoluble in dissolution media. The characteristic peak at  $2\theta$  of 16.66 ° for ibuprofen (dashed frame area in Fig.2) was selected for relatively qualitative analysis because the rest characteristic peaks were overlapped with that of octadecanol and GMS.

The spectra of ibuprofen microspheres were also shown in Fig. 2. The relative qualitative analysis showed that ibuprofen was still crystal in octadecanol and GMS based microspheres. As depicted in our previous study of acetaminophen microspheres, the drug crystals were dissolved in dissolution media, forming porous

structural architecture [29]. Therefore, it was inferred that ibuprofen crystals exposed on the surface of microspheres dissolved in water, influencing the structural architecture of microspheres, which was verified by SR- $\mu$ CT results in the later sections.

#### 3.4. Instant dissolution to mimic *in vivo* release

The instant dissolution tests within 10 min were investigated to mimic the *in vivo* release of ibuprofen indicating the taste-masking effects to ibuprofen microspheres (Fig. 3). The release behaviors of raw ibuprofen powders and microspheres were tested in distilled water and hydrochloric acid solution (pH = 1.20). It was observed that all microspheres were slowly released under the sink condition, less than 10% within 10 min, which could be related to the poor solubility of ibuprofen in corresponding media. In phosphate buffer (pH = 6.80 and 7.20) media as artificial saliva, the raw ibuprofen powders was released more than 90% within 10 min, which resulted into unpleasant tastes. However, all the ibuprofen microspheres exhibited sustained-release characteristics, namely 50%, 38% and 32% within 10 min at pH 6.80 and 58%, 41%, and 35% within 10 min at pH 7.20 for ACM, WCM and CCM, respectively. Compared with ibuprofen raw pharmaceutical material, ibuprofen microspheres were capable of retarding the release of ibuprofen in simulated human saliva, which could effectively mask the unpleasant taste. Especially at pH 7.20 media, CCM released 0.19%, 4.56%, and 9.41% at 10, 60, and 120 s, which were lesser than ACM (0.75%, 4.85%, and 13.01%) and WCM (1.12%, 7.2%, and 12.99%). The results illustrated that CCM had the best taste-masking effect.

#### 3.5. Scanning electron microscope

During the drug dissolution tests in phosphate buffer at pH 7.20, microspheres were collected at 0, 5 and 10 min for SEM detection. The microspheres were represented as non-released, partially-released and completely-released, respectively. There was no obvious difference in morphology among the microspheres before dissolution. It was also noted that there were no significant changes in the architectures of microspheres during dissolution test, owing to the fact that ibuprofen was melted and uniformly dispersed in the matrix by fine recrystallization resulting no large voids formation during drug dissolution.

### **3.6. Synchrotron radiation X-ray micro-computed tomography**

#### **3.6.1. Two-dimension monochrome X-ray micro-computed tomography images**

As depicted in Fig. 5, the large circular ring on the periphery was the tube used for loading microspheres. In the tube, size of the microspheres varied a lot owing to different longitudinal positions. The dark areas in microsphere were some small voids within microspheres which were believed to be air bubbles resulted during cooling processes of microspheres formation. There were more voids for ACM because of contact with large quantities of air in the cooling medium, which was more likely to form air voids during microspheres cooling process.

A poor sphericity was found for the ACM with rough surface. It was probably due to the longer freezing time for microspheres that was cooled by air than WCM and CCM. The microspheres, thus, became much deformed that was resulted from the collision of microspheres with each other or with stainless steel trays during cooling process. Meanwhile, due to rapid cooling in water or citric acid solution, better

sphericity and smoother surface were observed for the microspheres cooled by the corresponding media.

### 3.6.2. Visualization of the internal 3D structure

The reconstructed 3D tomographic images of ibuprofen microspheres demonstrated that the 3D morphology and distribution of voids within the microspheres were highly variable. As depicted in Fig.6, the roughest surface and the poorest sphericity could be seen in ACM. It was also demonstrated that there was a larger void in the center of microspheres surrounded by many smaller voids. The voids were small and heterogeneously distributed within WCM, but much bigger in CCM. These results were in accordance with those obtained from 2D monochrome X-ray CT images. The surface of CCM was smoother than the microspheres cooled by water because solubility of ibuprofen was higher in water than that in citric acid solution. This led to parts of ibuprofen crystals getting exposed on the surface of microspheres and dissolved into water, forming concave structure on the surface.

Herein, the internal 3D structure of microspheres was further investigated on the basis of structure parameters, such as area of surface, volume, specific surface area, diameter, box ratio, sphericity, radius ratio, Feret ratio, and porosity (Table 1), to deeply understand the mechanism of task-masking.

The structural parameters of microspheres were analyzed by Student's t-Test. Based on ANOVA, all three kinds of microspheres of ibuprofen were significantly different ( $P < 0.05$ ). WCM was greatly distinguished ( $P < 0.001$ ) from ACM for area of surface, volume, specific surface area, diameter, Feret ratio and porosity. And



CCM was greatly distinguished ( $P < 0.001$ ) from ACM for sphericity, Feret ratio and porosity, while all the structural parameters contributed to distinguish each ibuprofen microspheres.

The porosity here was defined as the proportion of voids within microspheres and conformed in the order of  $ACM > CCM > WCM$ . Box ratio was the ratio between the maximum and the minimum side length of the bounding box (box ratio value  $\geq 1$ ) and conformed in the order of  $ACM > WCM > CCM$ . Radius ratio referred to the ratio between the maximum and the minimum distance between the centroid pixel position and the perimeter of microspheres (radius ratio value  $\geq 1$ ) which was conformed in the order of  $ACM > WCM > CCM$ . The box ratio and the radius ratio could reflect the extent of the microspheres approaching the sphere: when the values close to 1, the microspheres are spherical. In summary, owing to longer freezing time and air in the cooling medium, irregular shape, rough surface with numbers of concave structure and a large number of voids were observed in ACM. Because of higher interfacial tension resulted in stable internal structure of microspheres congealed in citric acid solution, CCM had regular and rounder morphology, the smoothest surface and little volume of voids inside. Generally speaking, microspheres with regular shape and smoother surface had smaller surface area as well as slower dissolution rate than that in rough particles, thus to have taste-masking effects.

These results provided the structural evidences to the mechanism of drug release profiles discussed above. It was concluded that due to the irregular shape and rough surface with numbers of concave structure, the ACM were more likely to remain in

contact with dissolution media during the dissolution process. In contrast, CCM and WCM had the slowest release owing to the smoother surface, regular and round morphology. However, the drug release profiles were similar for three kinds of microspheres in distilled water and hydrochloric acid solution (pH = 1.20) because of poor solubility of ibuprofen at that condition. Compared with the structural architecture of microspheres, the solubility of ibuprofen was the main factor affecting the release behavior of microspheres. Overall, there was a strong correlation between cooling processes, structural architecture and release behavior of microspheres.

#### **4. Conclusion**

The same formula of oral dosage forms may have different effects on taste-masking due to the production process. With the application of SR- $\mu$ CT, the 3D morphology as well as internal architectures of ibuprofen microspheres were accurately quantified for each preparation methods. The effect of cooling processes on particle morphology and internal structure as well as their contributions to the taste-masking were revealed in this study. Thus, the structure evaluation provides a new approach for internal structure based optimization and rational design for taste-masking.

## Acknowledgements

The authors are grateful for the financial support from the National Natural Science Foundation of China (No. 81773645) and National Science and Technology Major Project (2017ZX09101001-006).

## Reference

- [1] Brniak W, Maslak E and Jachowicz R. Orodispersible films and tablets with prednisolone microparticles. *Eur J Pharm Sci* 2015; 75: 81-90.
- [2] Juluri A, Popescu C, Zhou L, et al. Taste masking of griseofulvin and caffeine anhydrous using kleptose linecaps DE17 by hot melt extrusion. *AAPS PharmSciTech* 2016; 17(1): 99-105.
- [3] Tiwari RV, Polk AN, Patil H, et al. Rat palatability study for taste assessment of caffeine citrate formulation prepared via hot-melt extrusion technology. *AAPS PharmSciTech* 2017; 18(2): 341-348.
- [4] Khor CM, Ng WK, Kanaujia P, et al. Hot-melt extrusion microencapsulation of quercetin for taste-masking. *J Microencapsul* 2017; 34(1): 29-37.
- [5] Campbell GA, Charles JA, Roberts-Skilton K, et al. Evaluating the taste masking effectiveness of various flavors in a stable formulated pediatric suspension and solution using the Astree (TM) electronic tongue. *Powder Technol* 2012; 224: 109-123.
- [6] Wu X, Onitake H, Haraguchi T, et al. Quantitative prediction of bitterness masking effect of high-potency sweeteners using taste sensor. *Sensors Actuat B-Chem* 2016; 235: 11-17.

- [7] Noorjahan A, Amrita B and Kavita S. In vivo evaluation of taste masking for developed chewable and orodispersible tablets in humans and rats. *Pharm Dev Technol* 2014; 19(3): 290-295.
- [8] Yuan J, Liu TT, Li HR, et al. Oral sustained-release suspension based on a novel taste-masked and mucoadhesive carrier-ion-exchange fiber. *Int J Pharm* 2014; 472(1-2): 74-81.
- [9] Samprasit W, Akkaramongkolporn P, Ngawhirunpat T, et al. Fast releasing oral electrospun PVP/CD nanofiber mats of taste-masked meloxicam. *Int J Pharm* 2015; 487(1-2): 213-222.
- [10] Nieddu M, Rattu G, Boatto G, et al. Improvement of thymol properties by complexation with cyclodextrins: In vitro and in vivo studies. *Carbohydr Polym* 2014; 102: 393-399.
- [11] Diego-Taboada A, Maillet L, Banoub JH, et al. Protein free microcapsules obtained from plant spores as a model for drug delivery: ibuprofen encapsulation, release and taste masking. *J Mater Chem B* 2013; 1(5): 707-713.
- [12] Sugiura T, Uchida S and Namiki N. Taste-masking effect of physical and organoleptic methods on peppermint-scented orally disintegrating tablet of famotidine based on suspension spray-coating method. *Chem Pharm Bull (Tokyo)* 2012; 60(3): 315-319.
- [13] Liu MX, Yin DP, Fu HL, et al. Double-coated enrofloxacin microparticles with chitosan and alginate: Preparation, characterization and taste-masking

- effect study. *Carbohydr Polym* 2017; 170: 247-253.
- [14] Stange U, Fuhrling C and Gieseler H. Taste masking of naproxen sodium granules by fluid-bed coating. *Pharm Dev Technol* 2014; 19(2): 137-147.
- [15] Yehia SA, El-Ridi MS, Tadros MI, et al. Phenylalanine-free taste-masked orodispersible tablets of fexofenadine hydrochloride: development, in vitro evaluation and in vivo estimation of the drug pharmacokinetics in healthy human volunteers. *Pharm Dev Technol* 2015; 20(5): 528-539.
- [16] Onofre F, Macleod G, Muley V, et al. An investigation into taste masking of paracetamol using Aquacoat (R) ECD applied via different granulation processes. *Int J Pharm* 2016; 511(2): 1145-1146.
- [17] Rogers TL and Wallick D. Reviewing the use of ethylcellulose, methylcellulose and hypromellose in microencapsulation. Part 2: Techniques used to make microcapsules. *Drug Dev Ind Pharm* 2011; 37(11): 1259-1271.
- [18] Mohamed-Ahmed AHA, Soto J, Ernest T, et al. Non-human tools for the evaluation of bitter taste in the design and development of medicines: a systematic review. *Drug Discov Today* 2016; 21(7): 1170-1180.
- [19] Bile J, Bolzinger MA, Vigne C, et al. The parameters influencing the morphology of poly( $\epsilon$ -caprolactone) microspheres and the resulting release of encapsulated drugs. *Int J Pharm* 2015; 494(1): 152-166.
- [20] Qazi F, Shoaib MH, Yousuf RI, et al. Lipids bearing extruded-spheronized pellets for extended release of poorly soluble antiemetic agent-Meclizine HCl. *Lipids Health Dis* 2017; 16:75.

- [21] Morkhade DM. Evaluation of gum mastic (*Pistacia lentiscus*) as a microencapsulating and matrix forming material for sustained drug release. *Asian J Pharm Sci* 2017; 12(5): 424-432.
- [22] Cheewatanakornkool K, Niratisai S, Manchun S, et al. Characterization and in vitro release studies of oral microbeads containing thiolated pectin-doxorubicin conjugates for colorectal cancer treatment. *Asian J Pharm Sci* 2017; 12(6): 509-520.
- [23] Taylor J, Taylor JRN, Belton PS, et al. Formation of kafirin microparticles by phase separation from an organic acid and their characterisation. *J Cereal Sci* 2009; 50(1): 99-105.
- [24] Cai Z, Lei X, Lin Z, et al. Preparation and evaluation of sustained-release solid dispersions co-loading gastrodin with borneol as an oral brain-targeting enhancer. *Acta Pharm Sinica B* 2014; 4(1): 86-93.
- [25] Yin X, Li H, Guo Z, et al. Quantification of swelling and erosion in the controlled release of a poorly water-soluble drug using synchrotron x-ray computed microtomography. *AAPS J* 2013; 15(4): 1025-1034.
- [26] Li HY, Yin XZ, Ji JQ, et al. Microstructural investigation to the controlled release kinetics of monolith osmotic pump tablets via synchrotron radiation X-ray microtomography. *Int J Pharm* 2012; 427(2): 270-275.
- [27] Liu RH, Yin XZ, Li HY, et al. Visualization and quantitative profiling of mixing and segregation of granules using synchrotron radiation X-ray microtomography and three dimensional reconstruction. *Int J Pharm* 2013;

445(1-2): 125-133.

- [28] Kajihara R, Noguchi S, Iwao Y, et al. Structural changes of polymer-coated microgranules and excipients on tableting investigated by microtomography using synchrotron X-ray radiation. *Int J Pharm* 2015; 481(1-2): 132-139.
- [29] Guo Z, Yin X, Liu C, et al. Microstructural investigation using synchrotron radiation X-ray microtomography reveals taste-masking mechanism of acetaminophen microspheres. *Int J Pharm* 2016; 499(1-2): 47-57.

### Figure captions

**Fig.1. TGA characteristics showed the stability of constitutions of microspheres.**

GMS: glycerin monostearate; ACM: air-cooling microspheres; WCM: water-cooling microspheres; CCM: citric acid solution microspheres.

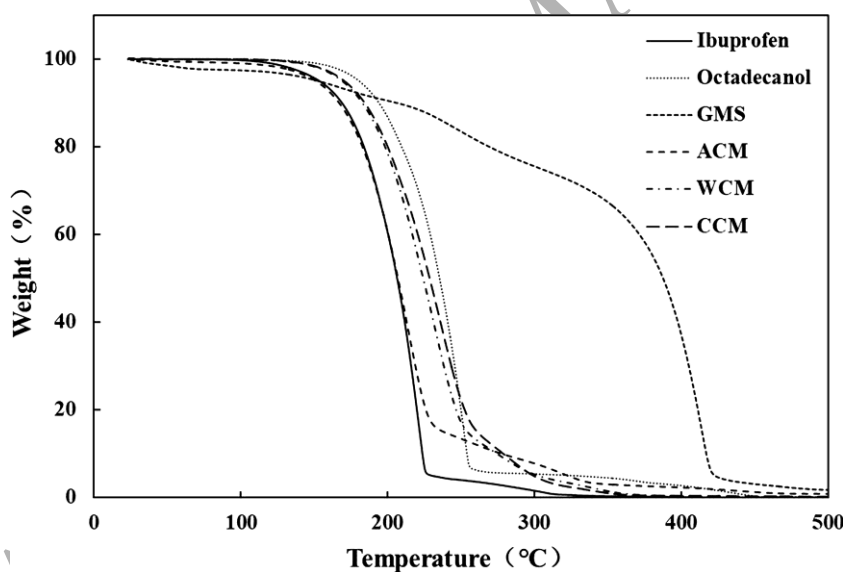


**Fig.2. XRD characteristics illustrated the components in microspheres.** GMS:

glycerin monostearate; ACM: air-cooling microspheres; WCM: water-cooling microspheres; CCM: citric acid solution-cooling microspheres.

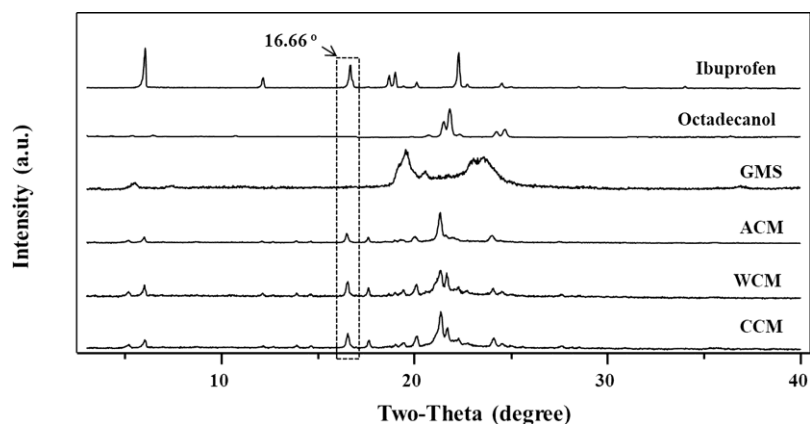


**Fig.3.** The *in vitro* dissolution profiles of ibuprofen microspheres indicated taste-masking efficacy. ●: ibuprofen; ■: air-cooling microspheres (ACM); ◆: water-cooling microspheres (WCM); ▲: citric acid solution-cooling microspheres (CCM).

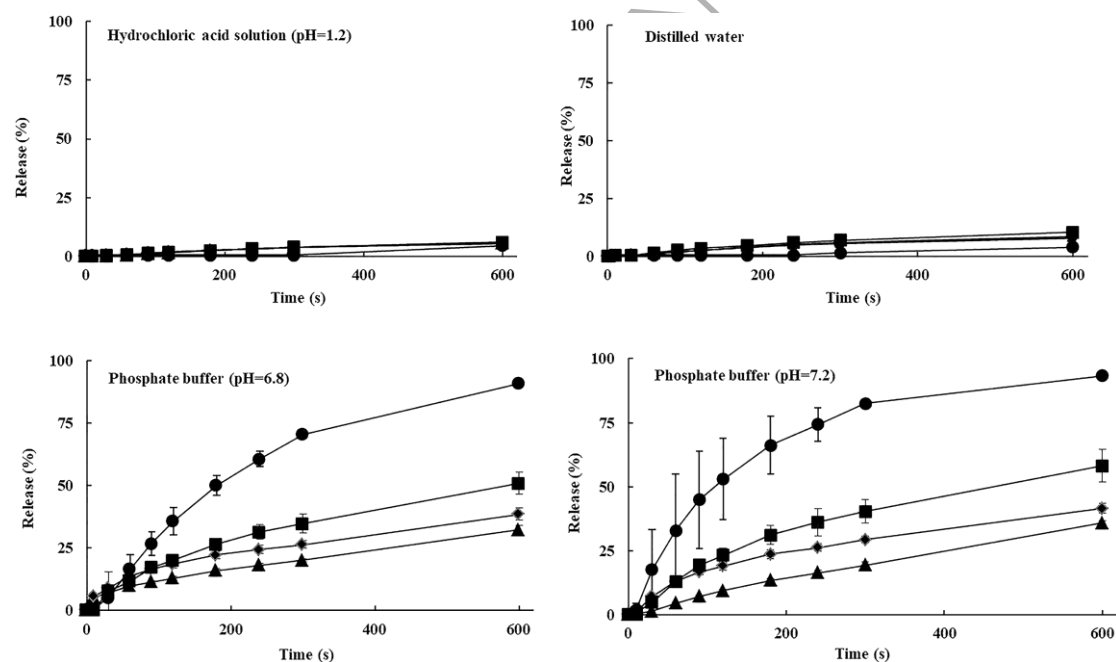


**Fig.4.** SEM characteristics demonstrated the morphology of ibuprofen microspheres at different sampling times. a, b, and c are images of air-cooling microspheres (ACM) at 0, 5, 10 min; d, e, and f are images of water-cooling microspheres (WCM) at 0, 5, 10 min; g, h, and i are images of citric acid solution-cooling microspheres (CCM) at 0, 5, 10 min.



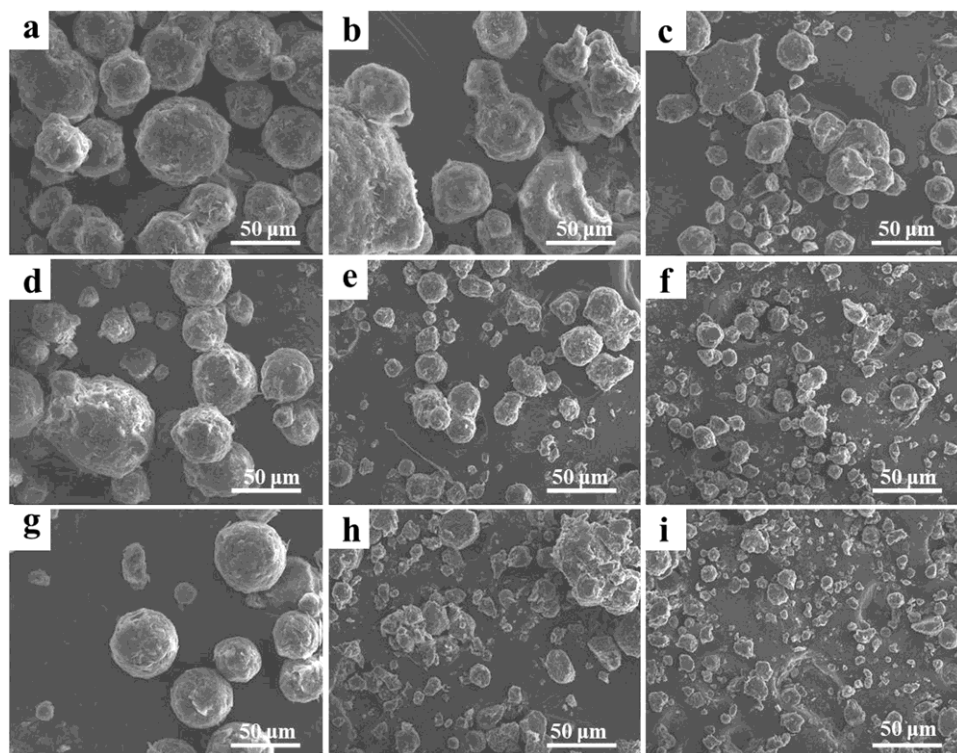


**Fig.5. 2D slice pictures of three kinds of ibuprofen microspheres.** a: air-cooling microspheres (ACM); b: water-cooling microspheres (WCM); c: citric acid solution-cooling microspheres (CCM).

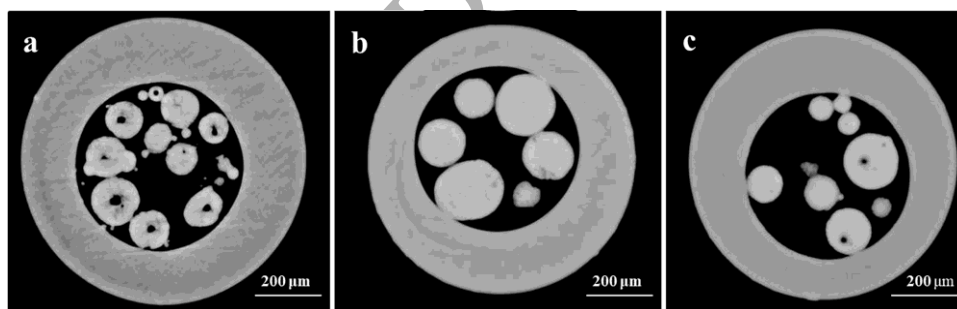


**Fig.6. 3D images of aggregate cavities of ibuprofen microspheres extracted after segmentation and related analysis.** a and d: 3D image and cavity of single air-cooling microsphere (ACM); b and e: 3D image and cavity of single water-cooling microsphere (WCM); c and f: 3D image and cavity of single citric acid solution-cooling microsphere (CCM).

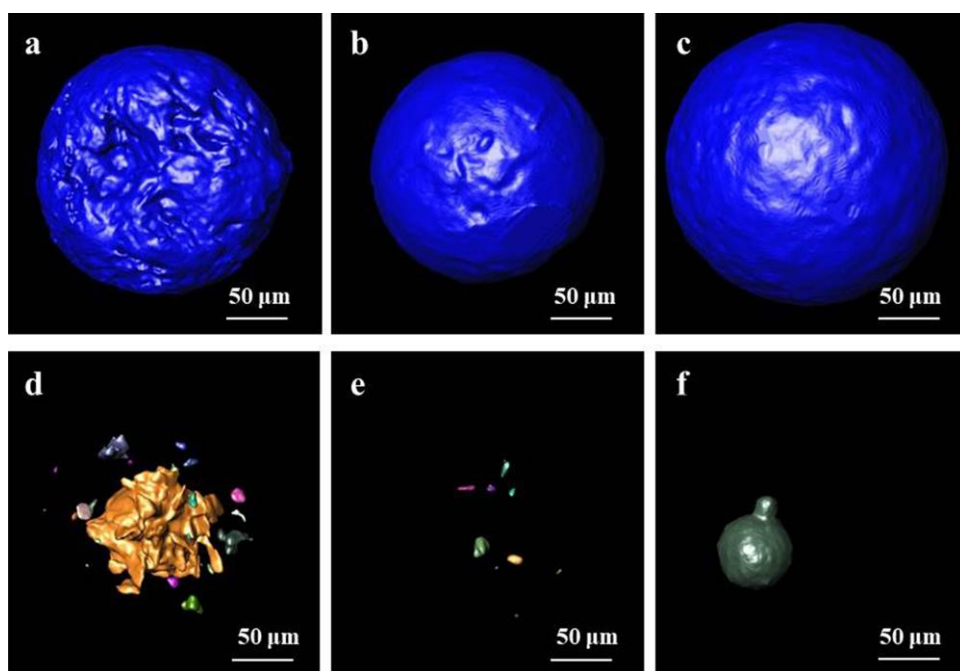


**Table 1 Structure parameters of the ibuprofen microspheres calculated by three-dimensional reconstruction technology.** ACM: air-cooling microspheres; WCM: water-cooling microspheres; CCM: citric acid solution-cooling microspheres. n = 30, mean  $\pm$  SD.

| Structure parameters                          | Samples             |                       |                     |
|---|---------------------|-----------------------|---------------------|
|   | ACM                 | WCM                   | CCM                 |
| Area of surface( $\mu\text{m}, \times 10^6$ ) | 7.16 $\pm$ 2.98     | 12.6 $\pm$ 1.69**     | 7.55 $\pm$ 3.88     |
| Volume( $\mu\text{m}, \times 10^9$ )          | 1.64 $\pm$ 0.826    | 3.82 $\pm$ 0.679**    | 2.05 $\pm$ 1.51     |
| Specific surface area                         | 0.0513 $\pm$ 0.0174 | 0.0333 $\pm$ 0.0022** | 0.0452 $\pm$ 0.0141 |
| Diameter                                      | 139.28 $\pm$ 34.47  | 193.14 $\pm$ 12.04**  | 147.78 $\pm$ 40.05  |
| Box ratio                                     | 1.06 $\pm$ 0.05     | 1.03 $\pm$ 0.02*      | 1.02 $\pm$ 0.02*    |
| Sphericity                                    | 0.91 $\pm$ 0.05     | 0.94 $\pm$ 0.03*      | 0.97 $\pm$ 0.01**   |
| Radius ratio                                  | 1.86 $\pm$ 0.72     | 1.81 $\pm$ 1.00       | 1.18 $\pm$ 0.07*    |
| Feret ratio                                   | 1.14 $\pm$ 0.07     | 1.07 $\pm$ 0.02**     | 1.07 $\pm$ 0.03**   |
| Porosity                                      | 3.294 $\pm$ 1.088   | 0.075 $\pm$ 0.071**   | 0.868 $\pm$ 0.628** |

ANOVA of the three samples,  $p < 0.05$ ; Compared with sample A by student's t-Test,

\* $P < 0.05$ , \*\* $P < 0.001$ .

## Graphical abstract

